ELSEVIER

Biochimica et Biophysica Acta 1460 (2000) 39–48

BIOCHIMICA ET BIOPHYSICA ACTA
BBA

www.elsevier.com/locate/bba

Review

Conformation and backbone dynamics of bacteriorhodopsin revealed by ^{13}C-NMR

Hazime Saitô *, Satoru Tuzi, Satoru Yamaguchi, Michikazu Tanio, Akira Naito

Department of Life Science, Faculty of Science, Himeji Institute of Technology, Harima Science Garden City, Kouto 3-chome, Kamigori, Hyogo 678-1297, Japan

Received 24 March 2000; accepted 24 March 2000

Abstract

It is demonstrated here how the secondary structure and dynamics of transmembrane helices, as well as surface residues, such as interhelical loops and N- or C-terminus of bacteriorhodopsin (bR) in purple membrane, can be determined at *ambient temperature* based on very simple ^{13}C-NMR measurements, together with a brief experimental background. In contrast to the static picture of bR, currently available from X-ray diffraction or cryo-electron microscopy, the structure consists of dynamically heterogeneous domains which undergo various types of local fluctuations with a frequency range of 10^2–10^8 Hz. The significance of this picture is discussed in relation to the biological function of this protein.

Keywords: Bacteriorhodopsin; Conformation; Dynamics; ^{13}C-NMR; Solid-state NMR; Conformation-dependent ^{13}C chemical shift

1. Introduction

Bacteriorhodopsin (bR) is a light-driven proton pump in the purple membrane of *Halobacterium salinarum*, consisting of seven transmembrane α-helices, with a retinal chromophore linked to Lys-216. The three-dimensional structure of bR has been determined by cryo-electron microscopy [1–3,7] and X-ray diffraction [4–6,8,9], and structures are also available for a few of the photointermediates [10,11]. These reported structures are very similar to one another in the dispositions of the transmembrane helices, but differ markedly, or are not well-defined, in the interhelical loops or N- or C-terminal domains. It appears that these are strongly influenced by the manner of sample preparation, such as the choice of two-dimensional or three-dimensional crystals and various environmental factors, such as ionic strength, temperature, etc. In order to relate the secondary structures to their functional roles under physiological conditions, a more detailed picture of bR, that includes the surface residues at *ambient temperature*, will be crucially important. Purple membrane sheets, that are formed in vivo, can be studied under such physiological conditions, and thus they will be free of perturbations. This is true especially if bR is considered as the prototype for a number of membrane proteins that mediate signal transduction, such as in G-protein-coupled receptors in which activation of G-proteins is triggered by recognition of external signals by these receptor molecules. So far, only fluorescence [12,13], spin- or heavy atom-label-

* Corresponding author. Fax: +81-7915-80182;
E-mail: saito@sci.himeji-tech.ac.jp

0005-2728/00/$ – see front matter
PII: S0005-2728(00)00128-6

ing techniques [14,15] have been utilized to examine the conformational features of the C-terminus and the loop regions, even though these methods are not free from perturbations from steric hindrance of the probes.

In principle, the NMR technique can be used as a versatile non-perturbing means to determine the structure and its fluctuations. In practice, solid-state NMR techniques are indispensable for membrane proteins to detect NMR signals arising from the anisotropic environment of the lipid bilayer [16–22]. A number of structural constraints are available from measurements of the relative orientation of several bond vectors with respect to the applied field in oriented system [16,17], or of interatomic distances as measured from partially recoupled dipolar interactions in unoriented samples [18,19]. These two approaches, suitable for smaller molecular systems, such as peptide fragments, are not always straightforward to apply to larger intact membrane proteins, such as bR, because of difficulties arising from severely overlapped signals, and uncertainties in bond angles and distances from time-averaging of the parameters for surface residues in the presence of motions.

Instead, we have explored an alternative, but very simple, approach to elucidate the conformation and the dynamics of ^{13}C-labeled intact membrane proteins, utilizing the available data base for the conformation-dependent displacement of ^{13}C chemical shifts [22–24]. Interestingly, the results reveal that the dynamic structure of bR is highly heterogeneous, dependent upon the domains of interest which fluctuate with frequencies from 10^2 to 10^8 Hz. Naturally, such native secondary structure of bR, including surface residues, varies with a variety of intrinsic or environmental factors, including site-directed mutagenesis, oligomerization of proteins, added cations, pH, temperature, extent of hydration, etc. This approach could then be extended to a study of a variety of membrane proteins, active in various types of biological functions.

2. Experimental background

2.1. Preparation of [^{13}C]-labeled bacteriorhodopsin

^{13}C-Labeled purple membranes of *Halobacterium salinarum* can be prepared by growing cells in a synthetic medium in which ^{13}C-labeled amino acids, such as [^{13}C]Ala, Val, or Leu were replaced with unlabeled ones, in order to raise the isotope level, from the 1.1% natural abundance up to 100% in the most favorable situation [25]. Alanine residues may be the best choice for the labeling site for ^{13}C-labeled proteins, because they are evenly distributed among the transmembrane helices (18 residues), loops (three residues) and N- and C-terminus (eight residues), and they have the lowest cost. In particular, [3- ^{13}C]Ala-labeling turned out to be the most suitable probe, better than [2-^{13}C] or [1-^{13}C]Ala labeling, because of the least possibility of isotope scrambling to other amino-acid residues [25], and of overlapping signals with those of natural abundance. Furthermore, the achieved spectral resolution with the latter labels was unexpectedly poor in the transmembrane α-helices, and the ^{13}C-NMR signals from interhelical loops were almost completely suppressed due to failure of peak-narrowing techniques from interference of internal motions to average chemical shift anisotropy with magic angle spinning, as will be described in more detail in Section 2.3 [26].

Recently, 12 well-resolved signals, including at least six single carbon signals, were resolved for the 22 Ala residues in the α-helices and loops of pelleted [3-^{13}C]Ala-bR samples, when the spectral resolutions were improved by increasing the sampling time of free induction decay from 25 to 50 ms [29] (Fig. 1C). Provisionally, these signals can be regiospecifically classified into three different domains, with reference to the conformation-dependent displacement of peaks for peptides and proteins, as will be discussed below [22–24]. At an earlier stage, only four broad signals could be resolved in lyophilized [3-^{13}C]Ala-bR samples (Fig. 1A), even though these samples were fully rehydrated by equilibration with environment of 100% relative humidity for 12 h [25,27]. This is because irreversible conformational distortion in peptide backbone might be caused by dehydration during lyophilization. Later, seven peaks were resolved when centrifuged pellets, instead of lyophilized samples, were used (Fig. 1B) [28].

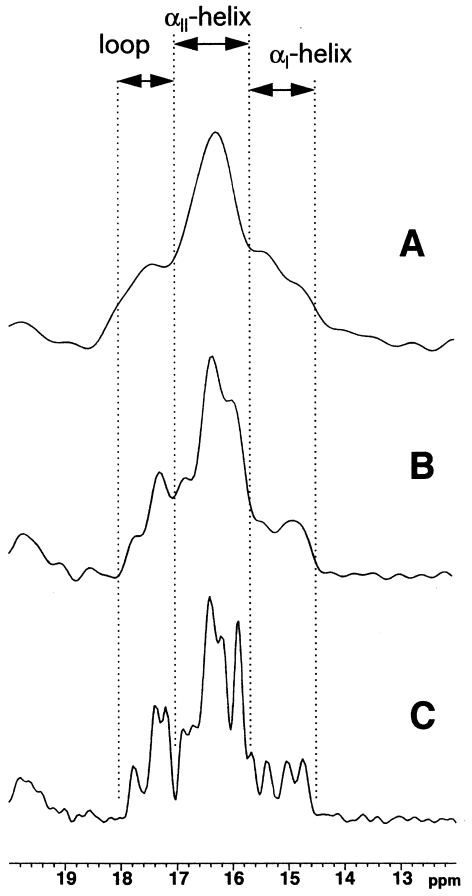

Fig. 1. ^{13}C-NMR spectra of [3-^{13}C]Ala-labeled bR under various conditions. (A) Lyophilized samples followed by hydration with equilibration under atmosphere of 100% relative humidity for 12 h [25]. (B) Centrifuged pellets, with sampling time 25 ms for free induction decay [27]. (C) The same sample with B, but sampling time was prolonged to 50 ms [28].

2.2. Local conformation determined by displacement of ^{13}C chemical shifts

It has been well-recognized that ^{13}C chemical shifts of the backbone C_α and carbonyl carbons as well as side-chain C_β signals of any amino acid residues in polypeptides and proteins are significantly displaced depending upon their local peptide conformations, defined by the torsion angles (ϕ and ψ), and the manner of hydrogen bonding of the former two types of carbons, irrespective of the peptide sequences [22–24]. Therefore, the local conformation of peptide chain can be conveniently determined from its ^{13}C chemical shift, with reference to accumulated data base summarized in Table 1, and at least six kinds of different local conformations can be distinguished for the Ala residues. *It is important to refer the ^{13}C chemical shifts in the solid state to the carboxyl peak of crystalline glycine at 176.03 ppm relative to TMS, if one aims to compare the given ^{13}C chemical shifts with those of the reference data* [22]. The observed conformation-dependent displacement of peaks is consistent with the calculated chemical shifts based on a theoretical calculation of ^{13}C chemical shifts for Ala C_β carbon from ^{13}C chemical shift contour maps using *N*-acetyl-*N*′-methyl-L-alanine amide as a model for Ala residue, although the effect of hydrogen bonding should be taken into account in the cases of the ^{13}C shifts of C_α and carbonyl carbons [30,31]. Naturally, ^{13}C chemical shifts of a normal α-helix (hereafter denoted as α_I-helix) were satisfactorily interpreted from the ^{13}C-NMR spectra of a number of fibrous proteins [22–24], and from synthetic transmembrane peptides of bR in homogeneous solution or solid-state cast from helix-promoting solvents [32]. In contrast, such peaks were displaced downfield to the peak positions of the α_{II} helices with reference to the ^{13}C chemical shifts of $(Ala)_n$ in hexafluoroisopropanol (HFIP) solution (Table 1), once these peptides are incorporated into a synthetic lipid bilayer, according to the definition of Krimm and Dwivedi [33]. The ^{13}C chemical shift of Ala C_β taking a turned structure located at the loop regions are resonated at lower field than the peak at 16.88 ppm of random coil [25,26,32].

Table 1
Conformation-dependent ^{13}C chemical shifts of Ala residues (ppm from TMS)

	α_I-helix[a]	α_{II}-helix[a]	α_L-helix[a]	β-sheet[a]	Collagen-like[a]	Silk I [a]	Random coil[b]
C_α	52.4	53.2	49.1	48.2	48.3	50.5	50.1
C_β	14.9	15.8	14.9	19.9	17.6	17.6	16.9
C=O	176.4	178.4	172.9	171.8	173.1	173.1	175.2

[a]Ref. [22].
[b]From the C-terminal tail of bR taken from Yamaguchi et al. [26,34].

The most important initial step in applying this NMR approach to membrane proteins is to assign the key ^{13}C-NMR peaks of bR, for instance, as in Fig. 1. Several approaches are possible, for instance, based on comparison of spectra between wild-type and site-directed mutants, which lack the specific residue under consideration, limited proteolysis, etc. For instance, the Ala-196 and -126 ^{13}C-NMR peaks were straightforwardly assigned to the peaks whose intensities were lost in the site-directed mutants, A196G and A126G, respectively, because no additional spectral change was noted by introduction of this sort of site-directed mutagenesis, as summarized in Table 2 [34]. The difference spectra between the wild-type and the A53G or A53V mutants were also very useful in the assignment of the Ala-53 signal, even though this particular peak was overlapped with other unassigned peaks [28]. It should be taken into account that there exists a possibility to induce an accompanied local conformational change as a result of site-directed mutagenesis, as in A103C or A39V [34]. Nevertheless, this approach remains effective if such an accompanied conformational change is local. This type of peak assignment was made easier in some cases when the superimposed signals from other residues could be removed. If these are located at a site to which Mn^{2+} ion can bind, the result of accelerated transverse relaxation due to the presence of Mn^{2+} ions will result in line-broadening [35].

Table 2
^{13}C chemical shifts of [3-^{13}C]Ala-, [1-^{13}C]Ala-, and [1-^{13}C]Val-labeled bR at 20°C (ppm) [34]

	Location	CH_3	C=O	Methods
Ala-39	Helix B	16.40		A39V
-51	Helix B	15.96		A51G, Mn^{2+} binding
-53	Helix B	16.3	177.9	A53G, A53V
-81	Helix C	16.52		A81G, Mn^{2+} binding
-84	Helix C	16.88		A84G
-103	C–D loop	17.20[a]		A103C
-126	Helix D	15.39		A126G
-160	E–F loop	17.38[a]		A160G
-196	F–G loop	17.78		A196G
-215	Helix G	16.20		A215G Mn^{2+}
-228,- 233	Helix G′	15.91		Limited proteolysis
-240, -244–246	C-terminal	16.88		Limited proteolysis
Val-49	Helix B		172.0	V49A
-69	B–C loop		173.0	Limited proteolysis
-199	F–G loop		171.1	V199A

[a]These peaks are displaced depending upon temperature.

It is noteworthy that some of the resonance peaks in lipid bilayer or purple membrane deviated from their expected peak positions from the torsion angles as determined at lower temperature by X-ray diffraction. For instance, Ala-84 signal is incidentally resonated at the peak position of random coil conformation (Table 2), although this peak was detected by the CP-MAS (cross polarization-magic angle spinning) spectra, that originate from residues undergoing anisotropic fluctuation. Therefore, it is more likely that this peak is accidentally overlapped with the boundary peak of 16.88 ppm between the lowermost end of the α-helices and other forms [32] as a result of local anisotropic motions rather than rigid body motions with rate constant in the order of 10–10^2 Hz [32]. In fact, the magnitude and direction of the observed displacement of peaks from α_I- to α_{II}-helices [36] are consistent with those of the calculated ^{13}C chemical shift based on the chemical shift contour maps [30,31], by taking into account of the predicted changes in the torsion angles [33]. Nevertheless, such torsion angles in the α-helices for bR did not deviate to the extent proposed by Krimm and Dwivedi [33], as revealed by cryo-electron microscope or X-ray diffraction at low temperatures [2–8]. So far, the presence of α_{II}-helix has been supported by a number of spectroscopic measurements performed at ambient temperature [33,37–39]. It is therefore most likely that such sequence-dependent displacement of ^{13}C-NMR peaks can be ascribed to local conformational fluctuation of Ala residues at ambient temperature around torsion angles typical of α-helices. The estimated α_{II}-helix content, as deduced from the carbonyl chemical shifts, is much lower as in the Ala C_β signals, probably because the carbonyl signal is more sensitive to the manner of hydrogen bonding than to such conformational fluctuations or deviations [31]. It is therefore, more appropriate to define the α_{II}-helix observed by NMR as a dynamically distorted helix, instead of statically distorted one, as previously proposed.

2.3. Detection of fast and intermediate motions

It should be recognized that not all the ^{13}C-NMR

signals of intact membrane proteins are always visible at ambient temperature. If there is an isotropic or large amplitude motion, whose correlation time is shorter than 10^{-8} s as in the case of the C-terminus end, it can be very easily identified from the selective suppression of CP-MAS signals from immobilized domains (blanked area **a**, corresponding to the high-frequency motion of 10^8 Hz) as compared with those of DD-MAS (dipolar decoupled-magic angle spinning) experiments which detect also mobile domains (see Fig. 2). This kind of motion can be also very easily detected by the observation of prolonged ^{13}C spin-lattice relaxation times as determined by DD-MAS experiments, illustrated by the horizontal bar in Fig. 2B [26,32]. In fact, this type of motion was first recognized at ambient temperature when the ^{13}C-NMR signals of the C-terminal residues were partially suppressed in the CP-MAS NMR spectrum, as compared with DD-MAS NMR spectrum. The latter is capable of detecting signals from whole area of protein in view of the relatively shorter spin-lattice relaxation times of Ala C_β carbons ($\sim$0.5 s) [26–28], provided that there is no additional *incoherent* random motion which results in interference with peak-narrowing by *coherent* proton decoupling or magic angle spinning process, as will be discussed below [40,41].

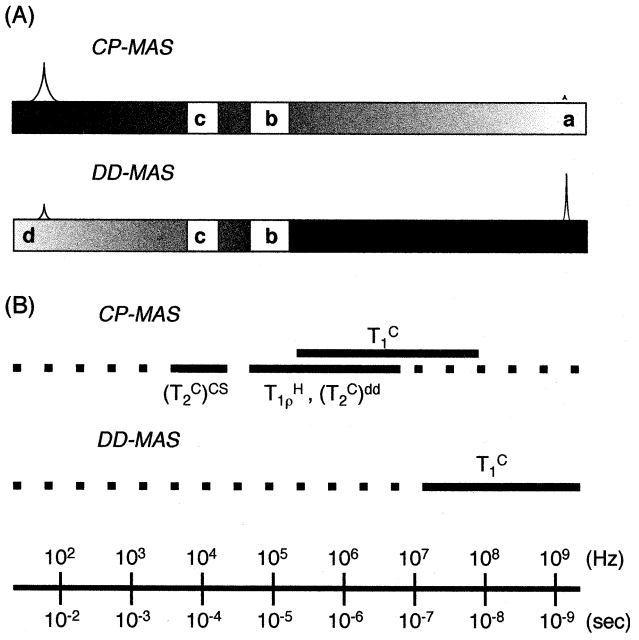

Fig. 2. Detection of several types of motions either by observation of suppressed peaks (A) or measurements of relaxation parameters (B) as a function of respective motional frequency (Hz) or its time scale or correlation times (s). NMR peaks were suppressed by: fast isotropic motion (**a**), interference with proton decoupling frequency (**b**), and magic angle spinning (**c**), and longer spin-lattice relaxation times as compared with repetition time (**d**). In the former, 'blanked area' means the time scale at which peak intensities are suppressed, whereas the horizontal bars in the latter indicate the correlation time which is most sensitive to the presence of motions, **a**, **b** or **c**.

It is emphasized that molecular motions of intermediate frequency, if any, with time scale (correlation time) of 10^{-5} s which can interfere with proton decoupling frequency (ca. 50 kHz) can be very easily detected when certain ^{13}C-NMR signals from both [3-^{13}C]Ala-labeled CP-MAS and DD-MAS NMR spectra are simultaneously suppressed (blanked area, **b**), as shown in Fig. 2A [40,41]. Such motion was first recognized when the ^{13}C-NMR signals of C-terminus were almost completely suppressed both in the CP-MAS and DD-MAS NMR, when temperatures were lowered to -40°C through -110°C [42]. This kind of peak suppression is also present at ambient temperature for interhelical loops and some transmembrane α-helices in [3-^{13}C]Ala-labeled bleached bacterio-opsin (bO) (see Fig. 3) [34], and in the M-like state of the D85N and D85N/D96N mutants [43] in which retinal–protein interaction was completely or partly removed either by removal of retinal or neutralization of negative charge at Asp-85, respectively. As illustrated in Fig. 3, the ^{13}C-NMR signals of Ala-160 and -196 in the E–F and F–G loops, respectively, and Ala-39, -53, -84 and -215 in helices B, C and G were suppressed as a result of acquired intermediate motions with correlation times of 10^{-5} s, instead of a plausible conformational change previously proposed [28]. In a favorable case, the presence of such motion can be detected by means of proton spin-lattice relaxation times in the rotating frame ($T_{1\rho}^{H}$) or carbon spin-spin relaxation times under CP-MAS condition $(T_2^C)^{dd}$ [44], as illustrated by the solid lines which indicate the most sensitive time scale shown in Fig. 2B. In fact, this type of motion was previously demonstrated for bO as measured by the proton spin-lattice relaxation times in the rotating frame [28]. This is the case in which carbon spin–spin relaxation time under proton CP-MAS condition is dominated by dipolar interaction (see Fig. 2B, the horizontal bar for $(T_2^C)^{dd}$).

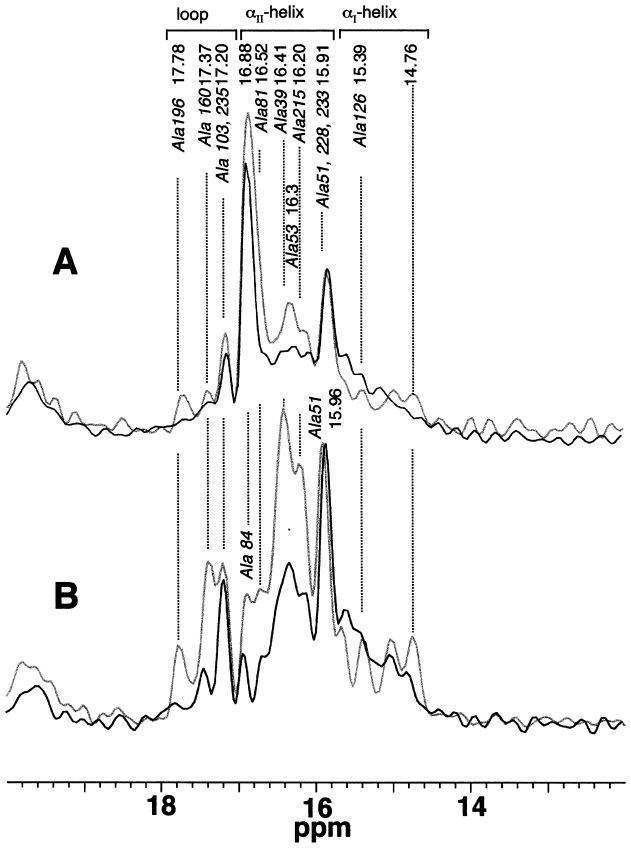

Fig. 3. ^{13}C-NMR spectra of bacterio-opsin (bO) (black peaks) as compared with those of bacteriorhodopsin (bR) (gray peaks) recorded by the DD-MAS (A) and CP-MAS (B) methods [34].

Furthermore, molecular motions with correlation times of 10^{-4} s, if any, could interfere with magic angle spinning in the order of 4 kHz, and result in suppression of ^{13}C-NMR signals of [1-^{13}C]- and [2-^{13}C]Ala-labeled bR and mutants (blanked area, **c**), [40,41] as shown in Fig. 2A. This is because the line-widths for the CP-MAS spectra determined by $(1/\pi T_2^{\varsigma})^{cs}$ [44]. In fact, it was demonstrated that the ^{13}C-NMR signal of transmembrane peptides labeled with the former probe was suppressed at ambient temperature because of the rigid-body motion of these helical peptides in the DMPC bilayer interfered with magic angle spinning [32]. Surprisingly, we also noticed that no spectral change was observed when ^{13}C-NMR spectra of [2-^{13}C]Ala-labeled proteins were compared among wild-type bR and its mutants at loop regions, such as A160G, A196G and A103C [26], although ^{13}C-NMR signals of the loop regions from [3-^{13}C]Ala-bR were clearly visible. This means that the suppression of the ^{13}C-NMR signals of the loop regions in [2-^{13}C]Ala-bR is caused by interference of random motion with correlation time in the order of 10^{-4} s with magic angle spinning frequency [40,41], which is essential for averaging in chemical shift anisotropy in the order of 3 kHz, as estimated from single crystalline alanine [45]. This finding implies that the turned structure of the interhelical loops is not rigid at ambient temperature as anticipated, but slowly fluctuates among various preferred local conformations with a correlation time in the order of 10^{-4} s. In other words, while examination of such motion from [3-^{13}C]Ala-probe was inconclusive because of rapid methyl rotation, use of this label for other purposes can be justified exactly because of its insensitivity to such interference.

Fortunately, the ^{13}C-NMR signals from the loop regions in [1-^{13}C]Val-labeled bR, Val-69 and -199 in the B–C and F–G loops, respectively, were not suppressed, probably because the correlation times of these loops might be shorter than 10^{-5} s because of the presence of nearby Pro residues [46]. As a result, the conformational change associated with formation of the M-like state was clearly distinguishable by the upfield displacement of peaks in the ^{13}C-NMR signals of Val-69 in the B–C loop and Val-49 in helix B [43].

3. Identification of C-terminal α-helix and its significance

The presence of an α-helical segment at residues 226–235, is easily located from the peak at 15.91 ppm, ascribable to Ala-228 and Ala-233 [27,36]. From its ^{13}C chemical shift (Table 1), this peak was naturally ascribed to an α_{II}-helix that protrudes from the membrane surface, at residues 226–235. It is demonstrated that this helix, anchored at the cytoplasmic surface, undergoes anisotropic fluctuation [36], as viewed from the conformation-dependent displacement of peaks. Only part of this α-helix was visible by X-ray diffraction [8] owing to the presence of motions with correlation time in the order of 10^{-6} s as judged from the carbon spin-lattice relaxation times (T_1^C) and spin–spin relaxation times under CP-MAS condition $(T_2^C)^{dd}$ [26]. This finding is consistent with the earlier hydrophobic fluorescent probe

experiment by Renthal and coworkers [13], who claimed that the C-terminal tail of bR is rigidly held at the membrane surface with motion on the time scale of 13–25 ns. Engelhard and coworkers [47] also demonstrated, on the basis of ^{13}C-NMR study of [3-^{13}C]- and [4-^{13}C]Pro-labeled bR, that the first part of the C-terminus is constrained. It was proposed that the C-terminus is fixed to the membrane via salt bridges between divalent cations and negative charges of the C-terminus as well as interhelical loops. In addition, Yamaguchi and coworkers found that this peak was stabilized when the temperature was lowered from 10 to −10°C, as a result of conversion from the α_{II}- to more stable α_I-helix form [36], consistent with our recent view that the former type of helix is present when helical segment is involved in local anisotropic motions [32].

In contrast with the wild-type, this C-terminal α-helix was shown to be destabilized at ambient temperature in some site-directed mutants, such as A160G. This is the result of rapid conformational fluctuation with correlation time of 10^{-8} s which specifically suppressed peaks in CP-MAS spectra, but they were recovered (correlation time in the order of 10^{-6} s) at temperatures between 10°C and 0°C, and again suppressed (10^{-5} s) below 0°C. Furthermore, deletion of the C-terminal helix by papain resulted in displacements of the peak positions in the loop regions such as Ala-160 or -103 [48]. These findings suggest that the C-terminus helix and the cytoplasmic loops strongly interact with each other to result in mutual stabilization, probably through electrostatic interaction or formation of a salt bridge [48]. It is rather surprising that a single-site mutation in the flexible E–F interhelical loop strongly affects the structure of the C-terminal helix and thereby the entire protein [48].

4. Heterogeneity in backbone dynamics

It is now clear that NMR picture of bR is highly heterogeneous from a dynamic point of view, with a distribution of correlation times between 10^{-2} and 10^{-8} s. The estimated correlation times of bR are: 10^{-2} s (transmembrane α-helices), 10^{-4} s (interhelical loops), 10^{-6} s (C-terminal α-helix), and 10^{-8} s (C-terminal tail). As described already, some loops and transmembrane α-helices in the bO or M-like state acquired accelerated motional freedom, to intermediate motion with correlation time in the order of 10^{-5} s, that allow conformational changes necessary for entry of retinal or conformational switch to result in the next steps in photocycle. In addition, it was already shown that site-directed mutation at the E–F loop resulted in rapid fluctuation of the C-terminal α-helix from 10^{-6} s to 10^{-8} s [48]. Undoubtedly, the presence of such flexible surface residues in intact bR at ambient temperature is the consequence of their location at the interface between the aqueous and lipid phases, and lack of any contact with the surface of another monomer as occurs in a three-dimensional crystal. This does not always mean, however, that these surface residues are completely disordered, because an α-helix structure protruding from the membrane surface can be readily recognized by the present NMR technique, in spite of a rigid body motion. In addition, any modifications of the cytoplasmic loop and the cytoplasmic end of some transmembrane helices are readily transmitted to each other through their interactions with the C-terminal α-helix [48]. This is also the main reason why positions of such surface residues cannot be accurately determined by X-ray diffraction or cryo-electron microscopy.

5. Effects of intrinsic or environmental factors on the overall structures of bR and bO

The present NMR approach is also very convenient for evaluating how the native conformation and dynamics of bR vary with environmental factors, such as temperature [42], pH [32,36,43], a variety of cations [28], ionic strength [42], and the in vivo or in vitro binding of retinal to bO [34]. As pointed out already, the ^{13}C-NMR signals from the C-terminal residues are suppressed at temperatures below −20°C, due to interference of motional frequencies with proton decoupling frequencies [27,42]. It was found that the well-resolved ^{13}C-NMR signals of bR in the presence of 10 mM NaCl at ambient temperature were broadened considerably at temperatures below −40°C, although no such change appears in the absence of NaCl [42]. This finding was interpreted in terms of chemical exchange among

peptide chains taking slightly different conformations with rate constant of 10^2 s^{-1} among several slightly different conformations at ambient temperature. At lower temperatures, these peaks are naturally broad, even without such chemical exchange process. That this exchange process was strongly influenced by the presence of sodium ion suggested that it plays an essential role in maintaining the secondary structure of bacteriorhodopsin, perhaps through re-organization of lipid molecules by partial screening of negative charge in the acidic head group of lipids [42]. Obviously, this kind of screening effect would arise from all types of mono- or divalent cations.

The native purple membrane has a considerably changed photocycle when cations are completely removed to yield the 'blue membrane'. As already demonstrated by ^{13}C-NMR spectra, the structure of bR is substantially modified in the blue membrane because of lowered surface pH [29]. Tuzi et al. therefore recorded ^{13}C-NMR spectra of [3-^{13}C]Ala-labeled 'sodium' purple membrane prepared by neutralization of acid blue membrane through titration of NaOH alone to search the exclusive binding site of divalent cations to bR. They showed that there are high-affinity cation-binding sites in both the extracellular and cytoplasmic regions, presumably near the surface and one of the preferred binding site is located at the F–G loop near Ala-196 of the extracellular side. Furthermore, the bound cations undergo rather rapid exchange among various types of cation binding sites [29].

6. Conformational changes through the proton transfer pathway

It was suggested that translocation of a proton from the cytoplasmic surface to the extracellular surface is associated with a protein conformational change [50,51]. It has been recognized that the first proton transfer in the photocycle of bR is from the protonated Schiff base to the anionic Asp-85, in the L to M reaction. This protonation induces the proton release from the proton release group containing Glu-194 and -204 at the extracellular surface, and might be linked also to the subsequent deprotonation of Asp-96 at the cytoplasmic region which causes the proton uptake. This means that the information of the protonation at Asp-85 should be transmitted to both the extracellular and the cytoplasmic regions, through specific interactions. Tanio et al. [46,52] recorded ^{13}C-NMR spectra of a variety of site-directed mutants in order to clarify how such interactions, if any, could be modified by changes of electric charge or polarity in mutants. This is based on the expectation that such interaction should also exist in bR even in the unphotolyzed state, among backbone, side-chains, bound water molecules, etc. They found that there is indeed a long-distance interaction between Asp-96 and extracellular surface through Thr-46, Val-49, Asp-85, Arg-82, Glu-204 and Glu-194 in the unphotolyzed state. For instance, conformational changes were induced at the extracellular region through a reorientation of Arg-82 when Asp-85 was uncharged, as manifested from the recovery of missing Ala-126 signal of D85N in the double mutant, D85N/R82Q [52]. The underlying spectral change might be interpreted in terms of the presence of perturbed Ala-126 mediated by Tyr-83 which is located between Arg-82 and Ala-126 [8]. It is possible that disruption of the above-mentioned interactions after protonation of Asp-85 in the photocycle could cause the same kind of conformational change as detected by the [3-^{13}C]Ala-labeled peaks of Ala-196 and Ala-126 [52] and also the [1-^{13}C]Val-labeled peaks of Val-49 and -199 [49].

Undoubtedly, this ^{13}C-NMR approach based on specific site-directed mutants will provide a valuable complementary means to X-ray diffraction, to clarify structure–function relationships at atomic resolution for a number of biologically important membrane proteins, in addition to bR, as demonstrated.

7. Conclusion and perspective

It is demonstrated that the non-perturbing ^{13}C-NMR approach of ^{13}C-labeled bR provides a detailed picture as to the conformation and the dynamics of this protein, and their changes due to various intrinsic and environmental perturbations, such as pH, temperature, metal ions, lipid composition, retinal, etc. at an *ambient temperature* of physiological relevance. In practice, the [3-^{13}C]Ala-labeled protein is the most appropriate from various points of view, as described in this review. These studies have shown

that bR is not a rigid system, as anticipated from the two-dimensional crystals in purple membrane, but undergoes several types of conformational fluctuations with frequency range from 10^8 to 10^2 Hz, depending on the respective domains under consideration and also influenced by a variety of intrinsic and environmental factors. The present approach also proved to be particularly useful to examine very flexible domains, such as surface residues protruded from the membrane surface, which are not amenable to crystallographic studies. In particular, it was found that the C-terminus α-helix plays an important role to stabilize the protein as a whole. Undoubtedly, this kind of a picture, together with the methodology used, will be a valuable approach for future studies of a variety of other membrane proteins including G-protein-coupled receptors.

Acknowledgements

The authors are indebted to Professor Janos K. Lanyi, University of California, Irvine, and Professor Richard Needleman, Wayne State University for their interest, extensive discussion and continued collaboration to pursue many of studies cited in this article. This work was supported, in part, by Grants-in-Aids for Scientific Research from the Ministry of Education, Science, Culture and Sports of Japan.

References

[1] R. Henderson, J.M. Baldwin, T.A. Ceska, F. Zemlin, E. Beckmann, K.H. Downing, J. Mol. Biol. 213 (1990) 899–929.
[2] N. Grigorieff, T.A. Ceska, K.H. Downing, J.M. Baldwin, R. Henderson, J. Mol. Biol. 259 (1996) 393–421.
[3] Y. Kimura, D.G. Vassylyev, A. Miyazawa, A. Kidera, K. Matsushima, K. Mitsuoka, K. Murata, T. Hirai, Y. Fujiyoshi, Nature 389 (1997) 206–211.
[4] E. Pebay-Peyroula, G. Rummel, J.P. Rosenbusch, E.M. Landau, Science 277 (1997) 1676–1681.
[5] H. Luecke, H.T. Richter, J.K. Lanyi, Science 280 (1998) 1934–1937.
[6] L. Essen, R. Siegert, W.D. Lehmann, D. Oesterhelt, Proc. Natl. Acad. Sci. USA 95 (1998) 11673–11678.
[7] K. Mitsuoka, T. Hirai, K. Murata, A. Miyazawa, A. Kidera, Y. Kimura, Y. Fujiyoshi, J. Mol. Biol. 286 (1999) 861–882.
[8] H. Luecke, B. Schobert, H.T. Richter, J.P. Cartailler, J.K. Lanyi, J. Mol. Biol. 291 (1999) 899–911.
[9] H. Berlhali, P. Nollert, A. Royant, C. Menzel, J. Rosenbusch, E.M. Landau, E. Pebay-Peyroula, Structure 7 (1999) 909–917.
[10] H. Luecke, B. Schobert, H.T. Richter, J.P. Cartailler, J.K. Lanyi, Science 286 (1999) 255–261.
[11] K. Edman, P. Nollert, A. Royant, H. Belrhali, E. Pebay-Peyroula, J. Hajdu, R. Neutze, E.M. Landau, Nature 401 (1999) 822–826.
[12] J. Marqhe, K. Kinoshita Jr., R. Gorindjee, A. Ikegami, T.G. Ebrey, J. Otono, Biochemistry 25 (1986) 5555–5559.
[13] R. Renthal, N. Dawson, J. Tuley, P. Horowitz, Biochemistry 22 (1983) 5–12.
[14] H.J. Steinhoff, R. Mollaaghababa, C. Altenbach, K. Hideg, M. Krebs, H.G. Khorana, W.L. Hubbell, Science 266 (1994) 105–107.
[15] M.P. Krebs, W. Behrens, R. Mollaaghababa, H.G. Khorana, M.P. Heyn, Biochemistry 32 (1993) 12830–12834.
[16] A.S. Ulrich, I. Wallat, M.P. Heyn, A. Watts, Nat. Struct. Biol. 2 (1995) 190–192.
[17] S.J. Opella, P.L. Stewart, Methods Enzymol. 176 (1989) 242–275.
[18] T. Gullion, J. Schaefer, J. Magn. Reson. 81 (1989) 196–200.
[19] D.P. Raleigh, M.H. Levitt, R.G. Griffin, Chem. Phys. Lett. 146 (1988) 71–76.
[20] L. Zheng, J. Herzfeld, J. Bioenerg. Biomembr. 24 (1992) 139–146.
[21] M. Engelhard, B. Bechinger, Isr. J. Chem. 35 (1995) 273–288.
[22] H. Saitô, S. Tuzi, A. Naito, Ann. Rep. NMR Spectrsc. 36 (1998) 79–121.
[23] H. Saitô, Magn. Reson. Chem. 24 (1986) 835–852.
[24] H. Saitô, I. Ando, Ann. Rep. NMR Spectrosc. 21 (1989) 209–290.
[25] S. Tuzi, A. Naito, H. Saitô, Eur. J. Biochem. 218 (1993) 837–844.
[26] S. Yamaguchi, S. Tuzi, H. Konishi, A. Naito, R. Needleman, J.K. Lanyi, H. Saitô, to be published.
[27] S. Tuzi, A. Naito, H. Saitô, Biochemistry 33 (1994) 15046–15052.
[28] S. Tuzi, S. Yamaguchi, A. Naito, R. Needleman, J.K. Lanyi, H. Saitô, Biochemistry 35 (1996) 7520–7527.
[29] S. Tuzi, S. Yamaguchi, M. Tanio, H. Konishi, S. Inoue, A. Naito, R. Needleman, J.K. Lanyi, H. Saitô, Biophys. J. 76 (1999) 1523–1531.
[30] I. Ando, H. Saitô, R. Tabeta, A. Shoji, Macromolecules 17 (1984) 457–461.
[31] I. Ando, S. Kuroki, H. Kurosu, M. Uchida, T. Yamanobe, ACS Symp. Ser. 732 (1999) 24–39.
[32] S. Kimura, A. Naito, S. Tuzi, H. Saitô, Biopolymers, in press.
[33] S. Krimm, A.M. Dwivedi, Science 216 (1982) 407–408.
[34] S. Yamaguchi, S. Tuzi, M. Tanio, A. Naito, J.K. Lanyi, R. Needleman, H. Saitô, J. Biochem. 127 (2000) 861–869.

[35] S. Tuzi, R. Kawaminami, A. Naito, R. Needleman, J.K. Lanyi, H. Saitô, manuscript in preparation.
[36] S. Yamaguchi, S. Tuzi, T. Seki, M. Tanio, R. Needleman, J.K. Lanyi, A. Naito, H. Saitô, J. Biochem. 123 (1998) 78–86.
[37] H. Vogel, W. Gartner, J. Biol. Chem. 262 (1987) 11464–11469.
[38] N.J. Gibson, J.Y. Cassim, Biochemistry 28 (1989) 2134–2139.
[39] J. Cladera, M. Sabes, E. Padros, Biochemistry 31 (1992) 12363–12368.
[40] J.S. Waugh, in: S.J. Opella, P. Liu (Eds.), NMR and Biochemistry, Marcel Dekker, New York, 1979, pp. 203–210.
[41] W.P. Rothwell, J.S. Waugh, J. Chem. Phys. 74 (1981) 2721–2732.
[42] S. Tuzi, A. Naito, H. Saitô, Eur. J. Biochem. 239 (1996) 294–301.
[43] Y. Kawase, S. Yamaguchi, M. Tanio, S. Tuzi, A. Naito, J.K. Lanyi, R. Needleman, H. Saito, manuscript in preparation.
[44] A. Naito, A. Fukutani, M. Uitdehaag, S. Tuzi, H. Saitô, J. Mol. Struct. 441 (1998) 231–242.
[45] A. Naito, S. Ganapathy, K. Akasaka, C.A. McDowell, J. Chem. Phys. 74 (1981) 3190–3197.
[46] M. Tanio, S. Inoue, K. Yokota, T. Seki, S. Tuzi, R. Needleman, J.K. Lanyi, A. Naito, H. Saitô, Biophys. J. 77 (1999) 431–442.
[47] M. Engelhard, S. Finkler, G. Metz, F. Siebert, Eur. J. Biochem. 235 (1996) 526–533.
[48] S. Yamaguchi, Ph.D. thesis, Himeji Institute of Technology, 2000.
[49] M. Tanio, S. Tuzi, S. Yamaguchi, H. Konishi, A. Naito, R. Needleman, J.K. Lanyi, H. Saitô, Biochim. Biophys. Acta 1375 (1998) 84–92.
[50] S. Subramaniam, M. Gerstein, D. Oesterhelt, R. Henderson, EMBO J. 12 (1993) 1–8.
[51] H. Kamikubo, M. Kataoka, G. Varo, T. Oka, F. Tokunaga, R. Needleman, J.K. Lanyi, Proc. Natl. Acad. Sci. USA 93 (1996) 1386–1390.
[52] M. Tanio, S. Tuzi, S. Yamaguchi, R. Kawaminami, A. Naito, R. Needleman, J.K. Lanyi, H. Saitô, Biophys. J. 77 (1999) 1577–1584.